

# Reductive sulfur biomineralisation in a re-flooded acid-sulfate soil landscape

Edward D. Burton<sup>A,B</sup>, Richard T. Bush<sup>A</sup>, Scott G. Johnston<sup>A</sup>, Leigh A. Sullivan<sup>A</sup> and Annabelle F. Keene<sup>A</sup>

<sup>A</sup>Southern Cross GeoScience, Southern Cross University, Australia.

<sup>B</sup>Corresponding author. Email ed.burton@scu.edu.au

## Abstract

We quantified the in-situ rates of dissimilatory  $\text{SO}_4^{2-}$ -reduction and the resulting S biomineralisation products in an acid-sulfate soil landscape which had been re-flooded by controlled tidal inundation.  $\text{SO}_4^{2-}$ -reduction was confined to the near-surface, formerly-drained soil layers and occurred at rates up to  $\sim 300 \text{ nmol/cm}^3/\text{day}$ . Elemental S was the dominant short-term product of  $\text{SO}_4^{2-}$ -reduction, and was present at up to  $\sim 40 \text{ } \mu\text{mol/g}$ . It was generally more abundant than iron-monosulfides or iron-disulfides in recently re-flooded soil layers. However, as expected, iron-disulfides were increasingly significant in soil layers that had experienced long-term inundation (i.e.  $40\text{-}80 \text{ } \mu\text{mol/g}$  formed over  $\sim 5$  years).

## Key Words

Acid-sulfate soils, elemental sulfur, iron, iron-sulfide, East Trinity.

## Introduction

The process of contemporary iron-sulfide formation in re-flooded acid-sulfate soils (ASS) consumes acidity and can sequester potentially-toxic trace elements (Burton *et al.* 2008a). Iron sulfide biomineralisation therefore offers an attractive site remediation outcome when drained ASS are inundated and reverted to wetlands. However, little quantitative information exists on either the in-situ rates of microbial dissimilatory  $\text{SO}_4^{2-}$ -reduction or the abundance of the resulting biomineralisation products during ASS wetland re-establishment. This limits the ability to accurately predict iron-sulfide biomineralisation, and to develop management strategies to optimise ASS remediation. The objective of this study was to examine reductive sulfur biomineralisation in a re-flooded ASS landscape that had been reverted to a tidal wetland. Specifically, we quantified the in-situ rates of dissimilatory  $\text{SO}_4^{2-}$ -reduction and the abundance of associated reduced inorganic S species in relation to tidal inundation.

## Methods

### Study site

The study site is an 800 ha coastal wetland located at East Trinity in north-eastern Australia. In the 1970's, a sea-wall with tide-gates was constructed in order to exclude tidal inundation and thereby drain the wetland soils. This caused iron-sulfide oxidation and severe acidification. In 2001-02, a program of lime-assisted tidal exchange was initiated in order to remediate the acidified soil layers. The tidal exchange component of this approach has involved incremental tidal inundation across the formerly drained site.

### Field methods and analyses

A transect was established at the tidal inundation front (Figure 1). Groundwater levels were measured using Odyssey (ODYPS05) pressure transducers, housed in 50 mm diameter PVC piezometers. Soil samples (0.1 m intervals, to 1.5 m below the soil surface) were collected at 5 positions along the transect using a gouge-auger. The samples were immediately transferred into 50 mL centrifuge vials with no headspace and stored at  $4^\circ\text{C}$  until return to our laboratory within 2-3 days. In-situ  $\text{SO}_4^{2-}$ -reduction rates were determined using the S-35 incubation method (Jakobsen and Postma 1999). This involved collecting undisturbed soil sub-samples using 3 mL polypropylene syringes with the distal end removed. These sub-samples were retrieved from an intact soil profile held within a gouge-auger. The samples were injected with 150 to 200 kBq of  $^{35}\text{SO}_4^{2-}$ , incubated at ambient temperature for 24 hrs and then mixed with 20% Zn acetate and frozen. The S-35 labelled samples were subjected to the 3-step RIS extraction procedure described below. The accumulation of S-35 in each RIS fraction was determined by liquid-scintillation counting.

Soil porewaters were recovered by centrifugation and analysed for pH, Eh,  $\text{Fe}^{2+}$  and  $\text{SO}_4^{2-}$  as per Burton *et al.* (2008a). Solid-phase Fe was extracted with deoxygenated 1 M HCl for 1 hour, followed by extraction with a citrate-buffered dithionite solution. The concentration of Fe(II) and Fe(III) in the 1M HCl, and total Fe in the dithionite extract were quantified via the 1,10-phenanthroline method. Solid-phase RIS species were

analysed using the 3-step extraction method of Burton *et al.* (2009). This involved (1) extraction of iron-monosulfides as acid-volatile sulfide (AVS) using 6 M HCl / 0.1M ascorbic acid (2) extraction of elemental S by shaking with toluene followed by quantification via HPLC, and (3) the recovery of iron-disulfides as Cr(II)-reducible S using the diffusion method of Burton *et al.* (2008b).

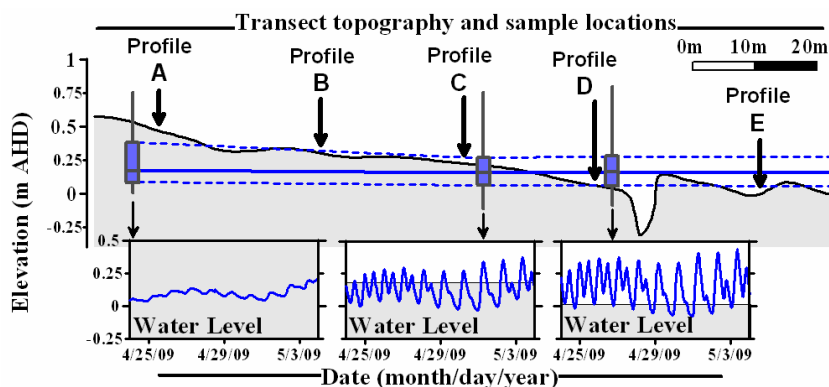


**Figure 1.** Topographic and hydrological features of the inundation-front transect. The blue line in the upper panel denotes the median groundwater level  $\pm$  the lower and upper quartile (interpolated from 3 piezometers, shown as the box-and-whisker plots). The solid-blue line in the lower panels shows the groundwater level, recorded at 30 minute intervals in each of the 3 piezometers.

## Results

The surface elevation of the transect studied here spanned  $< 0$  m to  $\sim 0.6$  m AHD. The median groundwater levels were 0.1-0.2 m AHD. However, these levels displayed significant short-term fluctuations due to tidal influence (Figure 1). At the lower end of the transect (i.e. near Profile E), the soil surface was for the most time covered by tidal surface waters. In contrast, towards the upper end of the transect, the soil surface was only infrequently inundated. The incremental nature of tidal inundation at the study site means that the transect reflects a temporal progression of increasing inundation duration from Profile E to Profile A. The near-surface depth intervals at Profile A and B had not been subject to considerable tidal inundation and had low pH and high Eh (Figure 2). In contrast, the whole soil profile at the lower end of the transect had experienced regular or continuous tidal inundation for  $> 12$  months. As a result, the pore water pH ranged from approx. pH 5 to 7 (Figure 2). This represents a substantial increase in pH when compared against the severely acidic conditions which existed prior to tidal inundation (Powell and Martens 2005; Johnston *et al.* 2009).

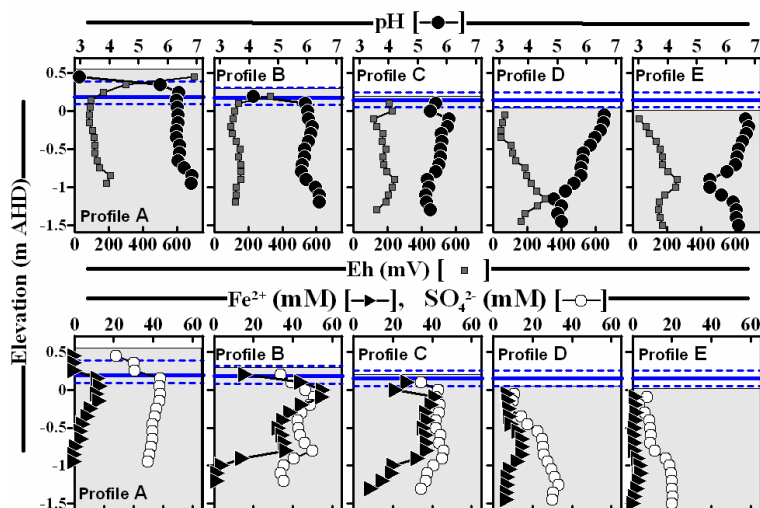


**Figure 2.** Selected porewater properties across the inundation-front transect. The blue lines show the median groundwater level (solid-line)  $\pm$  the lower and upper quartile (dashed lines).

The  $\text{Fe}^{2+}$  concentrations were extremely large (10 – 60 mM) within re-flooded soil layers (i.e. +0.1 to -0.7 m AHD) at Profile A, B and C (Figure 2). This is a result of reductive dissolution of Fe(III)-bearing minerals, such as jarosite, goethite and schwertmannite. The importance of Fe(III)-reduction is evident by the decreasing concentrations of both labile (1 M HCl-extractable) and crystalline (dithionite-extractable) solid-

phase Fe(III) in the surface 0 – 0.6 m depth intervals towards the lower end of the transect (Figure 3). This decrease is accompanied by increases in 1M HCl-extractable Fe(II) (Figure 3), which suggests that the low pore-water Fe<sup>2+</sup> concentrations in the 0 – 0.6 m depth interval at Profile D and E are due to precipitation of Fe(II) minerals such as siderite (FeCO<sub>3</sub>) and mackinawite (FeS).

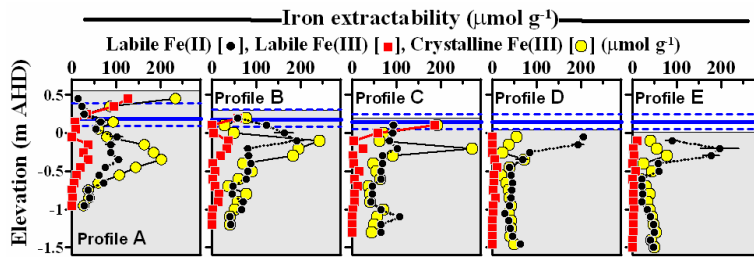


**Figure 3. Iron extractability across the inundation-front transect. The blue lines show the median groundwater level (solid-line) ± the lower and upper quartile (dashed lines).**

Within the un-oxidised estuarine sediment (below -0.7 to -0.9 m AHD), RIS speciation was dominated by FeS<sub>2</sub> (Figure 4). In the shallower, previously-drained soil layers, RIS speciation comprised a mixture of AVS, elemental S and FeS<sub>2</sub>. Given the site's history, the presence of RIS in these shallow soil layers is a consequence of recent reductive S biomineralisation. At Profile E (which has experienced prolonged and continuous tidal inundation over several years), FeS<sub>2</sub> was the most abundant RIS species, except in the surface 0 – 0.1 m depth interval. In contrast, elemental S and (to a lesser extent) AVS were the dominant biomineralisation products in the near-surface soil layers at Profiles A to D (see bottom panel in Figure 4).

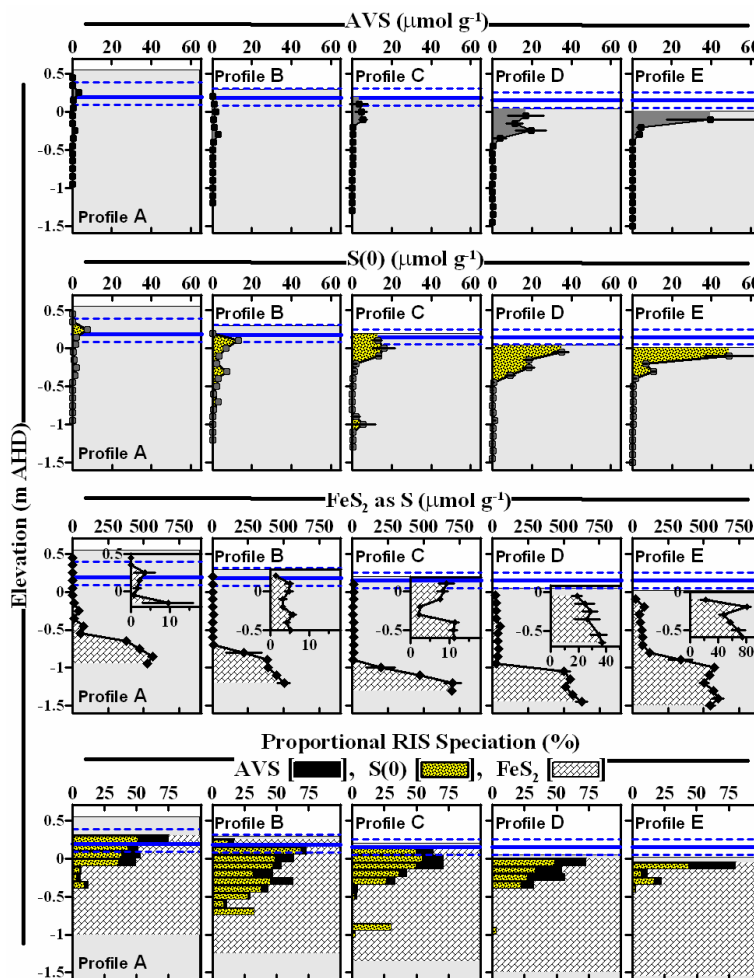


**Figure 4. Distribution of RIS species across the inundation-front transect. The blue lines show the median groundwater level (solid-line) ± the lower and upper quartile (dashed lines).**

In-situ SO<sub>4</sub><sup>2-</sup>-reduction was confined to the shallow, re-flooded soil layers (Figure 5). The rates were generally greatest near the soil surface, consistent with a ready supply of labile organic C. The exception to

this trend was the surface 0–20 cm depth at Profile A, which was above the upper quartile of groundwater level and thus still relatively oxidising (Figure 5). The actual rates of  $\text{SO}_4^{2-}$ -reduction were up to  $\sim 300 \text{ nmol/cm}^3/\text{day}$ , which is comparable to organic-rich salt marsh sediments. In terms of transect position, the rates were highest in the near-surface soil layers at Profiles B, C and D, and were lower towards both the upper (Profile A) and lower (Profile E) ends of the transect. At the upper end, this can be explained by the groundwater level being well below the O-horizon, which would limit the C supply necessary for  $\text{SO}_4^{2-}$ -reduction. In contrast, the  $\text{SO}_4^{2-}$ -reduction rates at the lower end of the transect (i.e. Profile E) appear to be limited by small pore-water  $\text{SO}_4^{2-}$  concentrations. Profile E is almost continuously inundated and as a consequence does not experience the same degree of  $\text{SO}_4^{2-}$  re-supply via tidal pumping that exists towards the middle of the transect (i.e. Profile C and D).

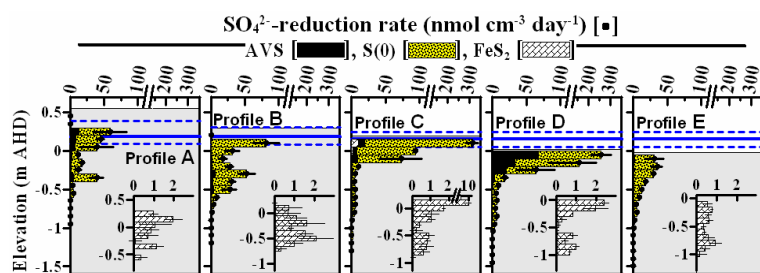


**Figure 5. In-situ rates of sulfate-reduction.** The blue lines show the median groundwater level (solid-line)  $\pm$  the lower and upper quartile (dashed lines).

Figure 5 shows that elemental S was the most important short-term product of  $^{35}\text{SO}_4^{2-}$ -reduction (Figure 5). The importance of elemental S as a short-term biomineralisation product is consistent with the abundance of elemental S in the shallow, formerly drained soil layers (bottom panel in Figure 4). In the soils examined here, the abundance of elemental S can be explained by oxidation of  $\text{H}_2\text{S}$  (the initial product released by  $\text{SO}_4^{2-}$ -reduction) by reaction with Fe(III) minerals (Burton *et al.* 2006).

Although not a major short-term product of  $\text{SO}_4^{2-}$ -reduction, the S-35 incubations provide strong evidence for rapid  $\text{FeS}_2$  formation in the shallow, formerly drained soil layers (see insets in Figure 5). Interestingly, this short-term formation of  $\text{FeS}_2$  was quite considerable at depths below the near-surface maximum in total  $\text{SO}_4^{2-}$  reduction rates. As a result, the contemporary accumulation of  $\text{FeS}_2$  is not concentrated near the soil surface, unlike the near-surface accumulation of AVS and elemental S (Figure 4).

## References

- Burton ED, Bush RT, Sullivan LA (2006) Elemental sulfur in drain sediments associated with acid sulfate soils. *Applied Geochemistry* **21**, 1240 – 1247.
- Burton ED, Bush RT, Sullivan LA, Johnston SG, Hocking RK (2008a) Mobility of arsenic and selected metals during re-flooding of iron- and organic-rich acid-sulfate soil. *Chemical Geology* **253**, 64 – 73.
- Burton ED, Sullivan LA, Bush RT, Johnston SG, Keene AF (2008b) A simple and inexpensive chromium-reducible sulfur method for acid-sulfate soils. *Applied Geochemistry* **23**, 2759–2766.
- Burton ED, Bush RT, Sullivan LA, Hocking RK, Mitchell DRG, Johnston SG, Fitzpatrick RW, Raven M, McClure S, Jang LY (2009) Iron-monosulfide oxidation in natural sediments: Resolving microbially-mediated S transformations using XANES, electron microscopy and selective extractions. *Environmental Science & Technology* **43**, 3128–3134.
- Jakobsen R, Postma D (1999) Redox zoning, rates of sulfate reduction and interactions with Fe-reduction and methanogenesis in a shallow sandy aquifer, Romo, Denmark. *Geochimica et Cosmochimica Acta* **63**, 137 – 151.
- Johnston SG, Keene AF, Bush RT, Burton ED, Sullivan LA, Smith D, Martens MA, McElnea AE, Wilbraham ST, van Heel S (2009) Contemporary pedogenesis of severely degraded tropical acid sulfate soils after introduction of regular tidal inundation. *Geoderma* **149**, 335 – 346.
- Powell B, Martens M (2005) A review of acid sulfate soil impacts, actions and policies that impact on water quality in the Great Barrier Reef catchments, including a case study on remediation at East Trinity. *Marine Pollution Bulletin* **51**, 149–164.